Indonesian Journal of Electrical Engineering and Computer Science
Vol. 7, No. 3, September 2017, pp. 625 ~ 642
DOI: 10.11591/ijeecs.v7.i3.pp625-642

Load Disturbance Rejection Based PID Controller for Frequency Regulation of a Microgrid

Badal Kumar*, Sandeep Bhongade
Electrical Engineering Department, S.G.S Institute of Technology & Science, Indore-03, India
*Corresponding author, e-mail: kumarbadal89@gmail.com

Abstract

Today's world is very much concerned to reduce green house gas emission from the conventional thermal power plants as cutting down emissions from transport and heating sector may not be realistic in the near future. To reduce pollution from electrical power sources, the world is now marching towards usage of renewable energy sources (RESs). These sources being small in capacity are mostly connected at the distribution voltage level. This indirectly reduces transmission and distribution losses as the sources are around the load. This distribution system having small scale energy sources is called as a microgrid or active distribution network. Microgrid operates generally in a grid connected mode. However, circumstances such as fault, voltage sag and large frequency oscillations in the main grid may force the active distribution network to be disconnected from the main grid and operate as an isolated microgrid. During this isolation there will be change in power output from the controllable microsources which are to be regulated properly to have a stable operation in regard to power balance and frequency of operation within the isolated microgrid. An autonomous isolated microgrid comprising both controllable & uncontrollable sources. Like solar, wind, diesel generator (DG), aqua electrolyzer (AE), fuel cell (FC), a battery energy storage system (BESS), and fly wheel (FW) are considered. Solar, wind, DG and FC are power generating source & BESS, FW, AE as energy storage element. The generated hydrogen by an AE is used as fuel for a FC. The power system frequency deviates for the sudden change in load demand and the real power generation. The output power of DG, FC, BESS, FW and power absorbed by AE is regulated by using controller such that frequency of the system is controlled. Controller used is proportional plus integral plus derivative (PID). Load Disturbance Rejection (LDR) is used for tuning of controller gains of the proposed hybrid system. This uses the chien-hornes-resnick (CHR) setting with 20% overshoot. Design of p-f droop (frequency regulation parameter) for different controllable source in microgrid using bode plot stability criterion. The system response with Modified LDR based controller, LDR based controller and classical controller are compared. Investigation shows that Modified LDR based controller gives best response amongst these three methods.

Keywords*: Load disturbance rejection, aqua electrolyzer, fuel cell, diesel generator, battery energy storage system, fly wheel, frequency and power deviation, integral and derivative control*

1. Introduction

In today's rapidly growing world, energy in any form is of ulmost importance. Among the different energy types, electric energy is one of the most important forms of energy and one cannot imagine the life without electric energy in these days. Traditionally, this energy requirement has been met by supplying the energy through long transmission and distribution networks which is generated at centralized generating stations. These generation stations use conventional source such as hydro, nuclear and polluting fossil fuels such as coal and diesel. Now-a-days, it has become a tough task to meet the requirements due to increasing demand as well as environmental constraints. Hence the people, including the engineers as well as policy makers, are looking at the new concept of the generation known as distributed generation (DG). DGs are small capacity generators, preferably uses renewable energy sources (RES), located at dispersed locations. The power generating sources in DG are called as distributed energy resources (DERs). These DGs interconnected together to form a power grid of smaller capacity, known as microgrid [1].

Generally, DGs are located in close proximity to the load/load centres, therby avoiding the long transmission and distribution networks to a great extent. The microgrid may operate in an autonomous mode or it can operate in a grid interconnected mode, decided by the operating

Received May 20, 2017; Revised July 25, 2017; Accepted August 11, 2017

conditions. Since, the concept of microgrid envolves many small capacity generators, may also be with variable power output, connected together necessitates highly coordinated operation among the different units to maintain the system stability [2, 3].

The various types of small scale generation systems used in a microgrid can be categorized into two groups namely primary sources consisting of solar and wind energy systems and secondary sources such as diesel generator, fuel cell, aqua electrolyzer, battery and flywheel [4, 6]. The solar and wind fall into the category of not correctly predictable energy sources in which the power varies with time i.e., not a constant power source. This results in power and frequency fluctuations in the microgrid. To overcome this problem secondary sources are used to supply power to balance out the increase in load demand or the reduction in power generation. However due to the delay in the output characteristics of secondary sources, the frequency oscillations are still present in the microgrid [7, 8]. Hence there is a need of designing proper controllers for secondary sources for optimal utilization of energy and to maintain minimum frequency deviations.

In the conventional Automatic Generation Control (AGC), it is well established that smaller the droop characteristics, lesser will be the frequency deviations. However, if the droop is larger, then there is a requirement for frequency bias term to be included in AGC as a secondary controller. In the past, the modelings of microgrid in the context of AGC has already been explained with controller gains and frequency bias decided through trial and error approach [9].

Method described in ziegler and Nichols has been used for the tuning of conventional PID controller [11]. The controller gains once tuned for a given operating point are only suitable for limited operating point changes. Therefore, the use of the conventional PID controller does not meet the requirements of the robust performance [12]. Basics of LDR are illustrated in MATLAB. The results of applying the LDR PID controller to the hybrid-power system are compared to those obtained by the application of a conventional PID controller. Simulated results show that the performance of the PID controllers tuned with modified LDR method is better than the LDR method than the classical method. Finally, the performance of the modified LDR controller has been concluded to be the best among the classical, LDR and modified LDR method [20].

The paper is described as follows. Section II illustrates Proposed hybrid System (Microgrid model) and its main components. Tuning of the PID controller by Modified LDR method and compared to LDRmethod and Classical method is presented in Section III. Section IV, explains the Simulation Results and Analysis are demonstrated under various condition. The conclusion is presented in Section V.

2. Proposed Hybrid System (Microgrid Model)

In this paper, we have considered a 100% self-sufficient isolated microgrid consisting of wind power source (300 kW), solar power source (300 kW), diesel generator (400 kW), fuel cell (200 kW), aqua-electrolyser (100 kW) and battery (30 kWh). The total generation from renewable sources and from the controllable sources is equal to 600 kW. The battery is used for supplying power only during transient period [10].

The block diagram of the proposed hybrid system is shown in Figure 1. The system consists of wind power source, solar power source, diesel generator, fuel cell, aqua electrolyzer, battery energy storage system and Fly Wheel. The power supplied to the load is the sum of output powers from wind and solar power source, diesel generator, fuel cell, battery energy storage system and fly wheel. The aqua electrolyzer is used to absorb the fluctuations of wind and solar power source and produce the hydrogen gas which is used as input to fuel cell generator. The mathematical models with first order transfer functions for fuel cell, aqua electrolyzer, BESS and Fly wheel & Second order for Diesel Generator are shown in this section [13].

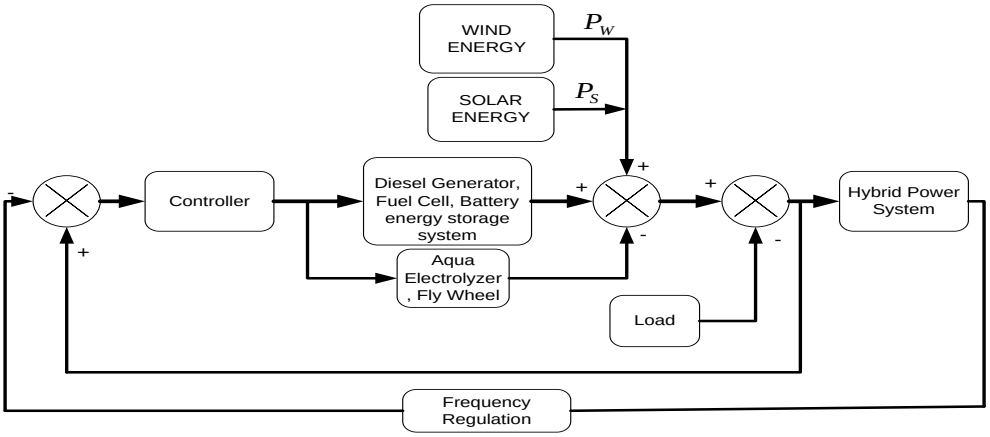

Figure 1. The block diagram of the microgrid with Primary sources, secondary sources and Hybrid power system

2.1. Wind Energy (Uncontrollable Source)

Usually maximum power point tracking (MPPT) is implemented in wind energy conversion system (WECS). However, because of this WECS loses its power output controllability. Hence, It cannot be used for frequency regulation of microgrid. In order to use WECS for this purpose we need to make some modifications in its control loops. Therefore in this paper we have treated the WECS as an uncontrollable source, not participating in frequency control. A constant power strategy is used in this paper [1, 2].

2.2. Solar Energy (Uncontrollable Source)

MPPT is also used in case of photovoltaic (PV) systems (as was in the case of WECS). Because of this, we do not have a control over the power output. Hence, in this paper the solar system is treated as an uncontrollable source, not participating in frequency control of the microgrid. A constant power strategy is used in this paper [1, 2].

2.3. Diesel Generator (Controllable Source)

Diesel generator can follow the load demand by means of its governor control and speed droop. The governor regulates the fuel input to an engine via a valve mechanism. The engine acts as a turbine and drives the synchronous generator. The governor of the diesel generator can be modelled with a first order transfer function [10], as depicted in (1).

$$G_{dg}(s) = \frac{1}{1+sT_{dg}} \tag{1}$$

Similarly, the turbine of the diesel generator can be modeled as presented in (2).

$$G_{dt}(s) = \frac{1}{1+sT_{dt}} \tag{2}$$

Therefore the overall transfer function of a diesel generator will be

$$G_{dgt}(s) = \frac{1}{1+sT_{dg}} \times \frac{1}{1+sT_{dt}} \tag{3}$$

Where T_{dg} , T_{dt} is the time constant of governor and turbine respectively.

2.4. Battery Energy Storage System (Controllable Source)

It is always an advantage if we are using RES to run power system instead of our conventional energy sources. One of the problems of using RES in power system operation is the fluctuation occurring in the amount of renewable energy obtained. Just for example, we won't be getting a steady flow of wind over a longer period of time. Similar fluctuation is also observed in case of solar energy(on an bright, sunny day one can expect high amount of solar energy, and on a cloudy day low level of solar energy would be obtained). Our prime objective of using secondary supply is to accommodate load fluctuation or/and primary source fluctuation. So any form of fluctuation in secondary storage is undesirable. Hence we cannot directly use RES as direct secondary supply. However, we all are aware about the advantage of RES over conventional energy sources. So to accommodate RES in the secondary supply side aan alternative method called aas BESS is used. The power generated from RES is stored inside a battery. This stored power is used to handle the load fluctuation and/or primary source fluctuation situation. From the battery we are able to get constant source of power without any fluctuation and also by this system we are able to use RES effectively. The transfer function model of battery energy storage system expressed by first order as [13] and implemented in microgrid as shown in Figure 3.

$$G_{BESS}(s) = \frac{1}{1+sT_{BESS}} \quad (4)$$

where T_{BESS} is time constant of battery energy storage system.

2.6. Fuel Cell (Controllable Source)

Power is produced in an fuel cell by the help of an electrochemical reaction between hydrogen and oxygen. One of the advantages of using fuel cell over conventional generators (like diesel generators) is that the energy produced is very pure and free from pollution. Usually a fuel cell produces a very small voltage which is not sufficient to meet our needs. In order to create large enough voltage, the cells are arranged in series-parallel combination to form a fuel cell stack. Hydrogen, which is used for power generation in fuel cell, is an expensive source as compared to other conventional energy sources. This is the only drawback of fuel cell[G]. Normally a fuel cell generator has a higher order model and also non-linearity. However during low frequency domain analysis we can be consider it to have a first order lag transfer function model given as [13] and implemented in microgrid as shown in Figure 5.

$$G_{fc}(s) = \frac{1}{1+sT_{fc}} \quad (6)$$

Where T_{fc} is time constant of fuel cell.

2.7. Aqua electrolyzer (controllable source)

In order to overcome this drawback we use aqua electrolyzer that produses hydrogen. Hydrogen is produces in aqua electrolyzer by method of "electrolysis of water" for which electric current is obtained from the power system. The transfer function model of aqua electrolyzer can be expressed by [13] and implemented in microgrid as shown in Figure 6.

$$G_{ae}(s) = \frac{1}{1+sT_{ae}} \quad (7)$$

where T_{ae} time constant of the AE. Since a typical AE consists of several power converters, time constant of the AE is very small [7].

2.8. Power and Frequency Deviations

In a power system consisting of synchronous generator, if the balance between the generation and load demand is not maintained, the frequency deviates depending on the domination of generation or load [17-19]. The power deviation is the difference between the power generation PG and the power demand PL. From the swing equation of a synchronous machine, the generator mathematical model can be written as:

$$\Delta f = \frac{f_{sys}}{2Hs}\left[\Delta P_G - \Delta P_e\right] \tag{8}$$

Where,

$$P_G = P_W + P_S + P_{dgt} + P_{fc} - P_{ae} \pm P_{bess} \pm P_{fw} \tag{9}$$

Generally, the loads are of mixed type like frequency dependant and non-dependant. So speed load characteristics of composite load is approximated by

$$\Delta P_e = \Delta P_L + D\Delta f \tag{10}$$

where the first term of (10) is the non-frequency dependent part of the load and the second term

$$\Delta P_G - \Delta P_L = \left(\frac{2H}{f_{sys}}s + D\right)\Delta f \tag{11}$$

Therefore the transfer function for system frequency variation to per unit power deviation is given by (12)

$$G_{sys}(s) = \frac{\Delta f}{\Delta P_G - \Delta P_L} = \frac{1}{D + \left(2H/f_{sys}\right)s} = \frac{K_{ps}}{1 + sT_{ps}} \tag{12}$$

where K_{ps} and T_{ps} are $1/D$ and $\left(2H/f_{sys}\right)$, respectively. It is to be noted here that (8) is valid only when there is a synchronous machine in the microgrid. Therefore the researchers should be careful in using (12) for simulating the microgrid [10].

2.9. Designing of P-F Droop for Different Controllable Source in the Microgrid

In the considered microgrid, there are three sources namely diesel generator, fuel cell and aqua electrolyzer with P–f droop. The P–f droop characteristics are required in the system when multiple power sources are connected in parallel like in microgrid [21, 22], [24, 25]. The individual power generators are responsible for maintaining the frequency. Conventionally, it is implemented as in (13)

$$\frac{m_2}{m_1} = \frac{P_{1rated}}{P_{2rated}} \tag{13}$$

Where m_1, m_2 are P–f droop coefficients and P_{1rated}, P_{2rated} are power ratings of generating sources in the microgrid. The above (13) is extended to microgrid sources as follows

$$R_{dg} : R_{fc} : R_{ae} : R_{bess} : R_{fw} = \frac{1}{P_{dgrated}} : \frac{1}{P_{fcrated}} : \frac{1}{P_{aerated}} : \frac{1}{P_{bessrated}} : \frac{1}{P_{fwrated}} \tag{14}$$

Where R_{dg}, R_{fc}, R_{ae}, R_{bess} and R_{fw} are p-f droop coefficient and $P_{dgrated}$, $P_{fcrated}$, $P_{aerated}$, $P_{bessrated}$ and $P_{fwrated}$ are rated power of diesel generator, fuel cell, aqua electrolyzer, Battery energy storage system and fly wheel respectively. Since the droops are related to the rating of the sources, at least one droop coefficient at the outset needs to be calculated and then droop coefficient for the generators need to be exercised. To start with, droop is calculated for the diesel generator, since the diesel generator has a second order transfer function which may lead to instability. The closed-loop signal flow graph of the diesel generator, fuel cell, aqua electrolyzer, battery energy storage system and fly wheel along with the hybrid power system is shown in Figure 7-11, respectively.

From Figure 7, open-loop transfer function of the diesel generator system can be as in (15)

$$G_{dg} = \frac{K_{hps}}{(1+sT_{dt})(1+sT_{dg})(1+sT_{hps})} \quad (15)$$

Similarly, the characteristic equation for the closed-loop system of Figure 7 will be

$$1+G_{dg}\times\frac{1}{R_{dg}} = 1+\frac{K_{hps}}{R_{dg}(1+sT_{dt})(1+sT_{dg})(1+sT_{hps})} \quad (16)$$

The signal flow graphs and bode plots corresponding to fuel cell, aqua electrolyzer, BESS and Fly wheel are shown in Figure 8-15, respectively

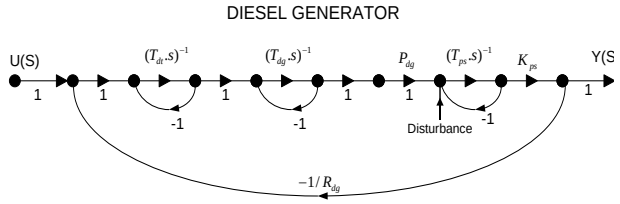

Figure 2. Signal flow graph of Diesel Generator along with Hybrid Power System

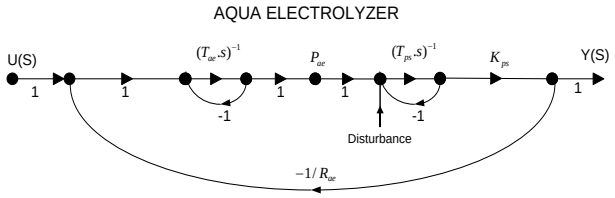

Figure 3. Signal flow graph of Aqua Electrolyzer along with Hybrid Power System

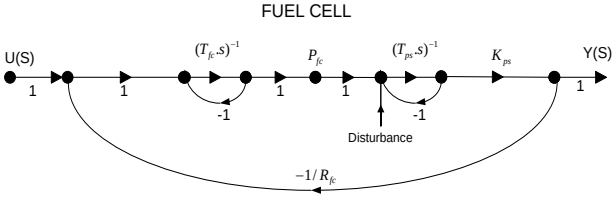

Figure 4. Signal flow graph of Fuel cell along with Hybrid Power System

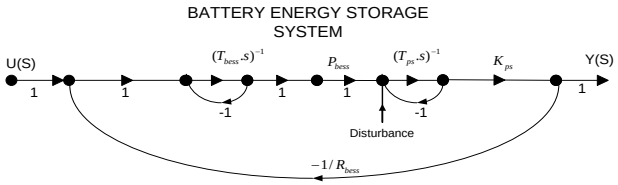

Figure 5. Signal flow graph of BESS along with Hybrid Power System

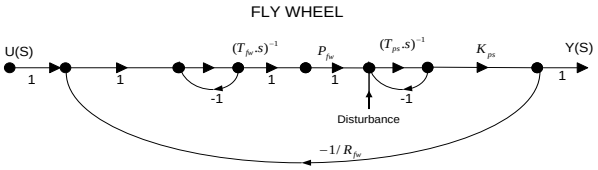

Figure 6. Signal flow graph of Fly wheel along with Hybrid Power System

The bode plot corresponding to G_{dg} and $G_{dg\_dr} = G_{dg}/R_{dg}$ of (15) is depicted in Figure 12. Figure 12 shows that if the droop is 'unity', the diesel generator along with the hybrid power system is unstable as both the phase and gain margins are negative. However, when the droop is 20.4918 the stability margin is well into the positive zone presenting a stable system. Further using (16) the P–f droop values of fuel cell (200 kW) and aqua electrolyzer (100 kW) are calculated and found to be 40.9836 and 0.002, respectively. And also p-f droop of battery energy storage system (30 KWh) and flywheel (30 KWh) are found to be 0.001[10].

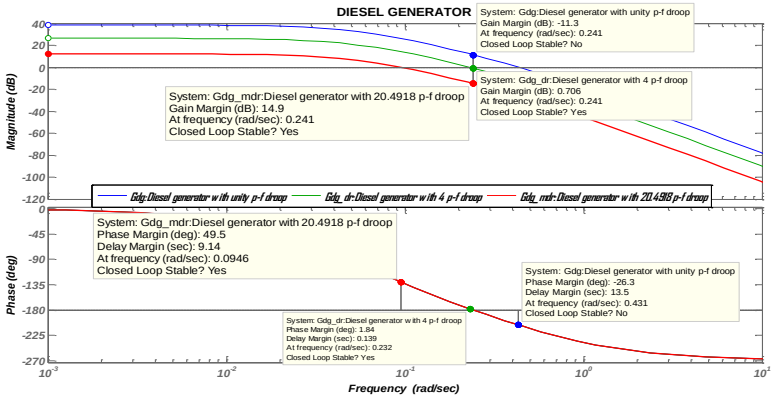

Figure 7. Bode Plot of Diesel Generator Along With Hybrid Power System and P-F Droop

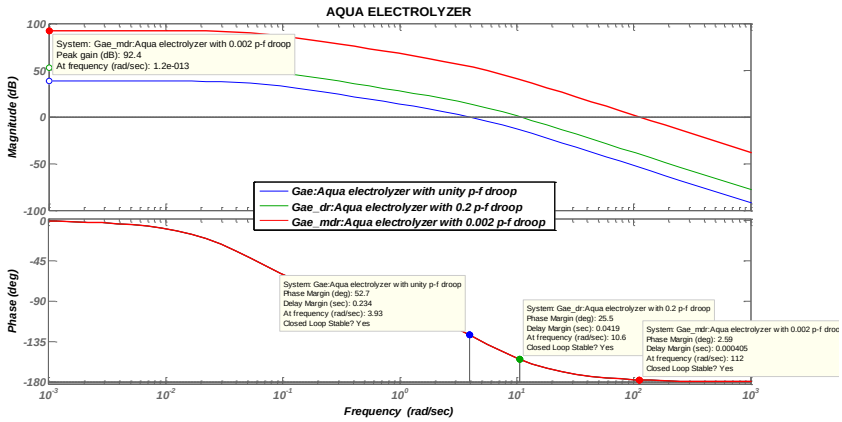

Figure 8. Bode Plot of Aqua Electrolyzer Along With Hybrid Power System and P-F Droop

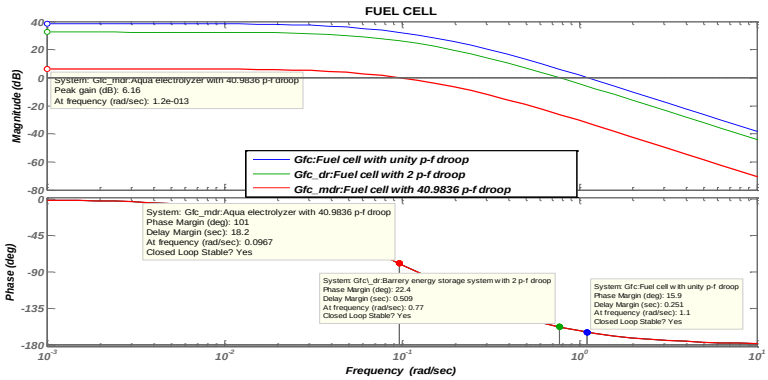

Figure 9. Bode Plot of Fuel Cell Along With Hybrid Power System and P-F Droop

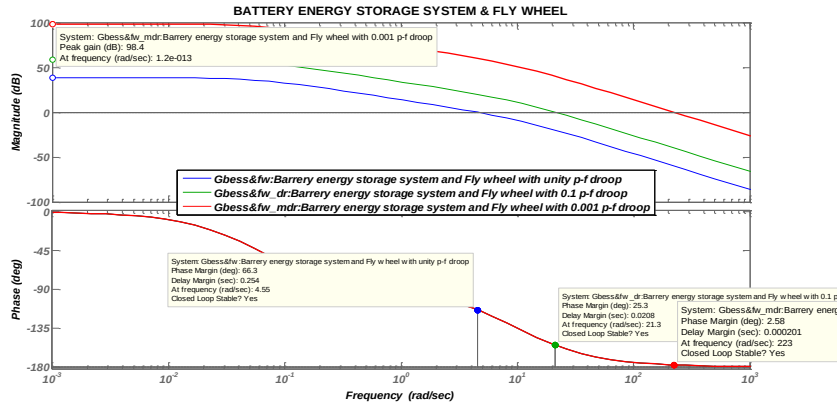

Figure 10. Bode Plot of BESS and Fly Wheel Along With Hybrid Power System and P-F Droop

In the above bode plot; we observe that all the secondary systems are stable because its phase margin and gain margin are positive. It also gives the value of droop.

3. Tuning of PID Controller Gain

The objective of the controllers is to regulate the power output of secondary sources, to minimize the frequency deviation by generating appropriate control signals and hence to enhance the performance of the microgrid. In the presence of many secondary sources there is a chance of adverse interaction between their regulators which leads to deterioration of frequency stability of the microgrid. So far there is no single definition for best tuning that applies to all loops. Therefore, to avoid the adverse interaction there is a need of appropriate tuning of the individual PID controller [13], [23].

In the present work SISO toolbox is used for PID tuning (PID controller is used because there is a need to improve both transient and steady state response).To generate this compensator Ziegler-Nichols open loop is used as a tuning algorithm with LDR as tuning preference. This method uses the Chien-Hrones-Resnick (CHR) setting with 20% overshoot. It is worth mentioning here that Ziegler-Nichols closed loop cannot be applied to first-order or second-order systems with time delay. If Ziegler-Nichols closed loop is selected for these cases, the tuning algorithm will automatically be switched to Ziegler-Nichols open loop [20].

Frequency bias factor is selected at which ITSE (Integral time square error) is minimum [13]. This can be represented as shown in Equation (17).

$$ITSE = \int_0^t t|\Delta f|^2 dt \quad (17)$$

In Classical method values of all the parameters (K_p, K_i, K_d and frequency bias) have been considered from the previous literature [13].

Table 1. Tuning of PID Controller Gains According To Classical Method

Microgrid Components	Frequency Regulation K_f	K_p	K_i	K_d
Diesel Generator	4	0.0397	0.0756	3.3084
Aqua Electrolyzer	0.2	0.35	0.03	0.07
Fuel Cell	2	0.1220	0.2154	3.1608
Battery	0.1	0.4188	0.01666	0.01
Fly wheel	0.1	0.3654	0.01666	0.01

In LDR method we are taking frequency regulation parameter is same as classical method but K_p, K_i and K_d values calculated from tuning preference Load disturbance rejection from MATLAB(SISO toolbox) [20].

Table 2. Tuning of PID Controller Gains According to LDR Method

Microgrid Components	Frequency Regulation K_f	LDR K_p	LDR K_i	LDR K_d
Diesel Generator	4	0.1025	0.0073	0.3013
Aqua Electrolyzer	0.2	1.498	4.5399	0.1044
Fuel Cell	2	0.1858	0.0464	0.156
Battery	0.1	3.380	0.1251	0.098
Fly wheel	0.1	3.380	0.1251	0.098

In Modified LDR method the gain values K_p, K_i and K_d were obtained from LDR method and changing the frequency regulation parameter from Bode plot stability criterion [10][22][24].

Table 3. Tuning of PID Controller Gains According to Modified Ldr Method

Microgrid Components	Frequency Regulation K_f	ModifiedLDR K_p	ModifiedLDR K_i	ModifiedLDR K_d
Diesel Generator	20.4918	0.1025	0.0073	0.3013
Aqua Electrolyzer	0.002	1.498	4.5399	0.1044
Fuel Cell	40.9836	0.1858	0.0464	0.156
Battery	0.001	3.380	0.1251	0.098
Fly wheel	0.001	3.380	0.1251	0.098

4. Simulation Analysis

The Detailed block diagram of the microgrid is shown in Figure 16 and its implementation in MATLAB/SIMULINK. The analysis was carried out by running the system for 200 sec. During this time the system was put under power variation in load as well as in sources. Before creating disturbance in all the cases, constant wind power supply of approximately 0.3 p.u., solar power supply of 0.3 p.u. and a load demand of 0.6 p.u. are considered. The time period shown in some plots is the different from the simulation time since in those cases the system is settling before the simulation time [10].

Case 1: The load is increased from 0.6 p.u. to 0.65 p.u. and the wind (0.3 p.u.) and solar power (0.3 p.u.) sources are kept constant for a time period of 50 sec. (Time Domain Analysis)

Time	T=0 sec	T=50 sec
Wind power	0.3 p.u.	0.3 p.u.
Solar power	0.3 p.u.	0.3 p.u.
Load demand	0.6 p.u.	0.65 p.u.

Due to the load variation the microgrid elements(i.e. secondary sources) are giving their dynamic performance and are shown in Figure 11(a)-(h).In the transient period the BESS and fly wheel are supplying the power in such a manner that when BESS is supplying power, fly wheel is charging and vice versa. The fluctuation in the power System frequency is due to the sudden change in the load demand and the PID controller is used to control the frequency deviation. The outputs of system components are automatically adjusted to corresponding value to minimize the error in supply demand and the frequency deviation. The gain values of PID controller obtained through classical, LDR and Modified LDR technique and are given in Table 1, Table 2 & Table 3 respectively.

From Figure 11(a) we observe that, the settling time using classical method, LDR method and Modified LDR method are 160 sec., 35 sec. and 20 seconds respectively for frequency regulation. It can be observed from Figure 11(b), that the settling time using Modified LDR method is 15 seconds and the settling time obtained from LDR method and classical method is 35 and 110 seconds respectively for regulation of power.

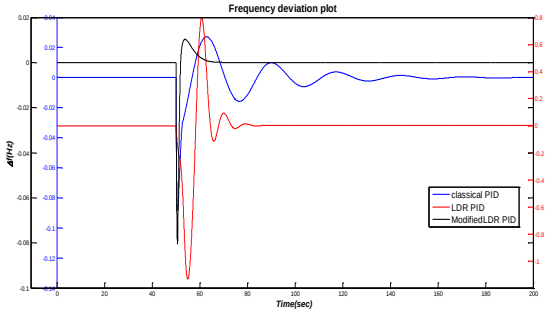

Figure 11(a). Frequency Deviation of Microgrid (Case 1)

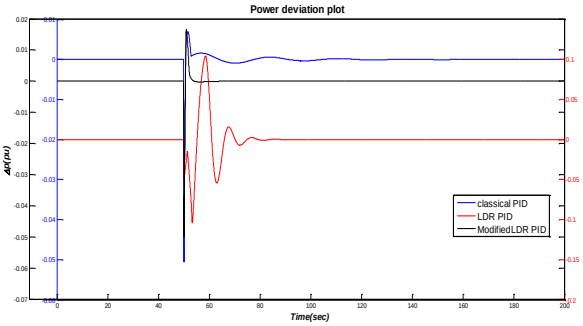

Figure 11(b). Power Deviation of Microgrid (Case 1)

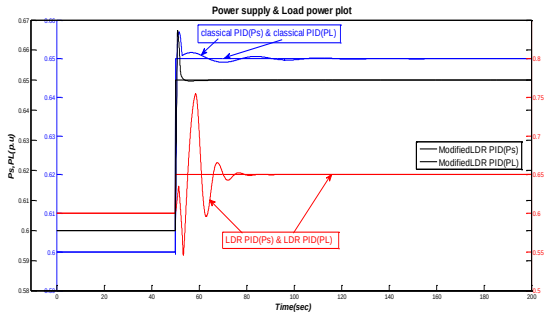

Figure 11(c). Supply Power and Load Power of Microgrid (Case 1)

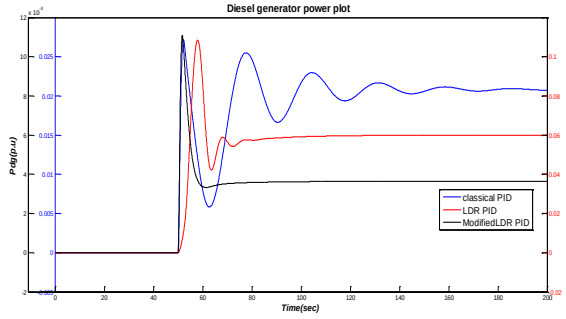

Figure 11(d). Contribution of Diesel Generator Power in Microgrid (Case 1)

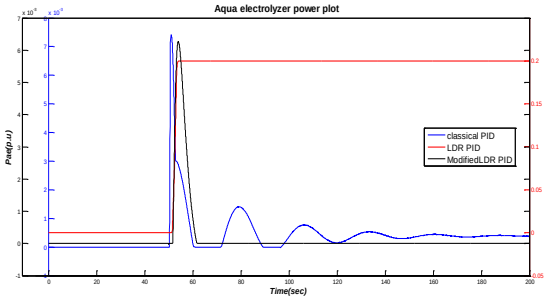

Figure 11(e). Contribution of Aqua Electrolyzer Power in Microgrid (Case 1)

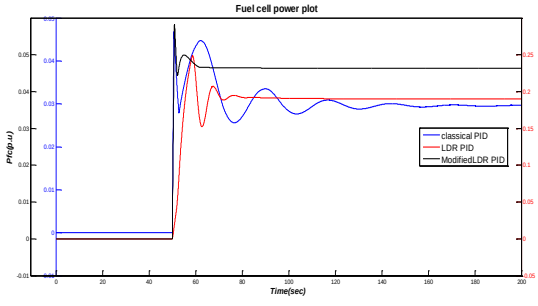

Figure 11(f). Contribution of Fuel Cell Power in Microgrid (Case 1)

From Figure 11(c) we observe that, the Modified LDR gives faster response as compared to LDR and classical methods. At steady state period, contribution of diesel generator is 0.02 p.u. at 175 sec, 0.06 p.u. at 80 sec and 0.004 p.u. at 60 sec. for Classical method, LDR method and Modified LDR method respectively to compensate the difference in load power of 0.05 p.u. this has been shown in Figure 11(d). The contribution of Aqua electrolyzer is negligible; it is used to generate Hydrogen for fuel cell only. This has been shown in Figure 11(e). From Figure 11(f), the fuel cell is contributing 0.03 p.u. power in 175 sec for classical method whereas 0.02 p.u. in 70 sec and 0.046 p.u. in 20 sec for LDR method and Modified LDR method respectively to compensate the difference in load power of 0.05 p.u. for frequency regulation.

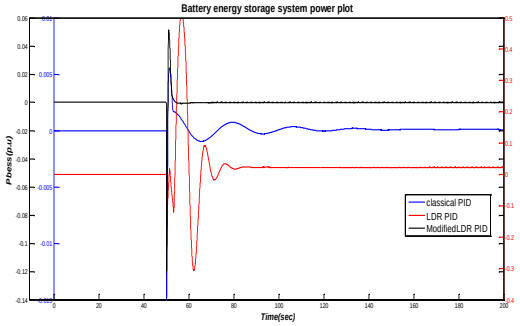

Figure 11(g). Contribution of BESS Power in Microgrid (Case 1)

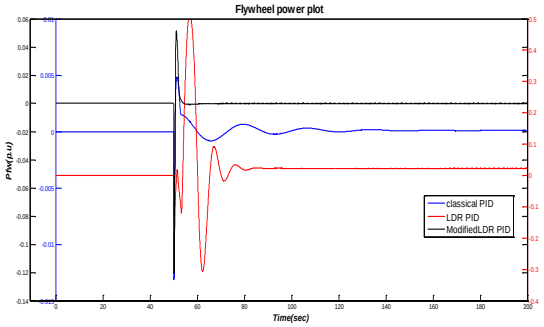

Figure 11(h). Contribution of Fly Wheel Power in Microgrid (Case 1)

From Figure 11(g) & Figure 11(h), we observed that the contribution of BESS and Fly wheel is only for transient period. From the simulation results as obtained in Figure 11(a)-(h), it is shown that the dynamic behavior of the proposed system gives better output as compared to the classical method and LDR method.

Case 2: The wind power and solar power are varied from 0.3 p.u. to 0 p.u. (worst condition) and load demand is increased from 0.6 p.u. to 0.65 p.u. for a time period of 50 sec. (Time Domain Analysis)

Time	T=0 sec	T=50 sec
Wind power	0.3 p.u.	0 p.u.
Solar power	0.3 p.u.	0 p.u.
Load demand	0.6 p.u.	0.65 p.u.

Due to the solar power,wind power and load variation the microgrid elements(i.e. secondary sources) are giving their dynamic performance and are shown in Figure (12(a)-12(h). The fluctuation in the power System frequency is due to the sudden change in the Renewable energy sources power and load demand and the PID controller is used to control the frequency deviation. The outputs of system components are automatically adjusted to corresponding value to minimize the error in supply demand and the frequency deviation. The gain values of PID controller obtained through classical, LDR and Modified LDR technique and are given in Table 1, Table 2 & Table 3 respectively.

From Figure 12(a) we observe that, the settling time using classical method, LDR method and Modified LDR method are infinite, 110 sec and 68 seconds respectively for frequency regulation.

It can be observed from Figure 12(b), that the settling time using Modified LDR method is 50 seconds and the settling time obtained from LDR method and classical method is 118 sec. and infinite respectively for regulation of power.

From Figure 12(c) we observe that, the Modified LDR gives faster response as compared to LDR and classical methods.

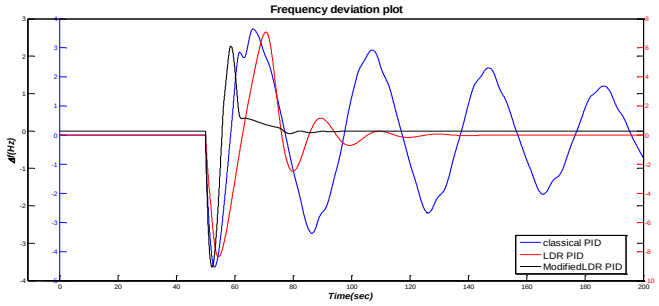

Figure 12(a). Frequency Deviation of Microgrid (Case 2)

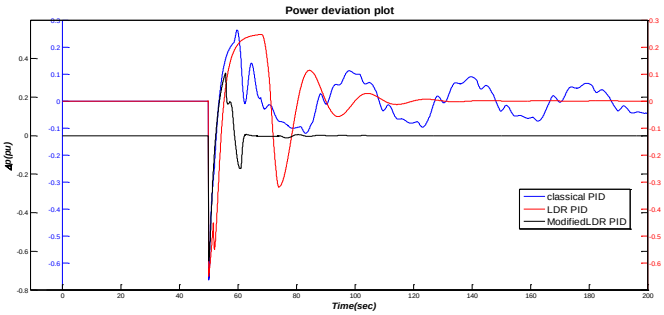

Figure 12(b). Power Deviation of Microgrid (Case 2)

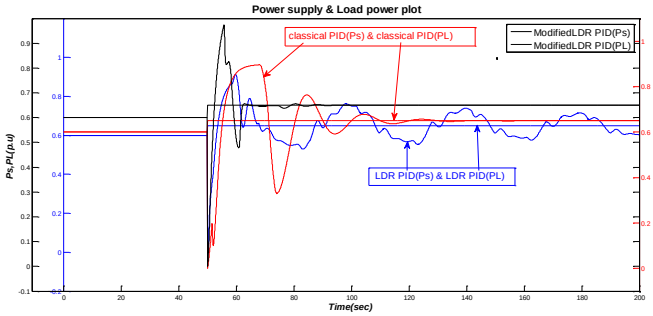

Figure 12(c). Supply Power and Load Power in Microgrid (Case 2)

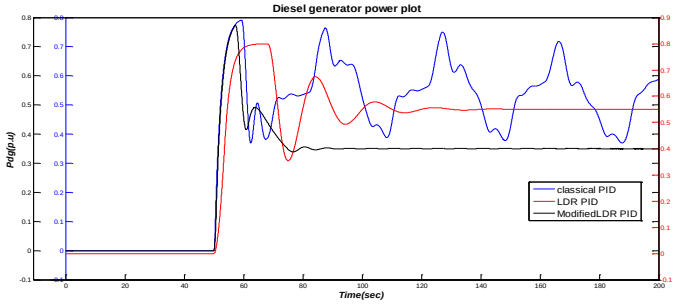

Figure 12(d). Contribution of Diesel Generator power in Microgrid (Case 2)

At steady state period, contribution from diesel generator is 0.35 p.u. at infinite, 0.50 p.u.at 100 sec and 0.35 at 45 sec for Classical, LDR and Modified LDR method respectively to compensate the difference in load power of 0.65 p.u. This has been shown in Figure 12(d).

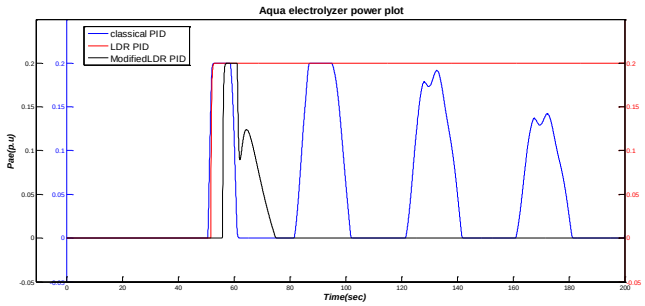

Figure 12(e). Contribution of Aqua Electrolyzer Power in Microgrid (Case 2)

The contribution of Aqua electrolyzer is negligible, it is used to generate Hydrogen for fuel cell only. This has been shown in Figure 12 (e).

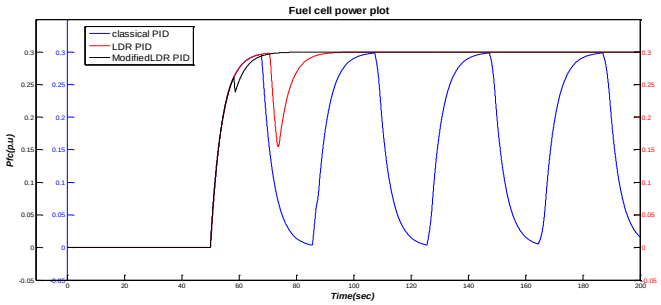

Figure 12(f). Contribution of Fuel Cell Power in Microgrid (Case 2)

From Figure 12(f), the fuel cell is contributing 0.3 p.u. power in infinite for classical method whereas 0.3 p.u. in 50 sec. and 0.3 in 28 sec for LDR method and Modified LDR method respectively to compensate the difference in load power of 0.65 p.u. for frequency regulation.

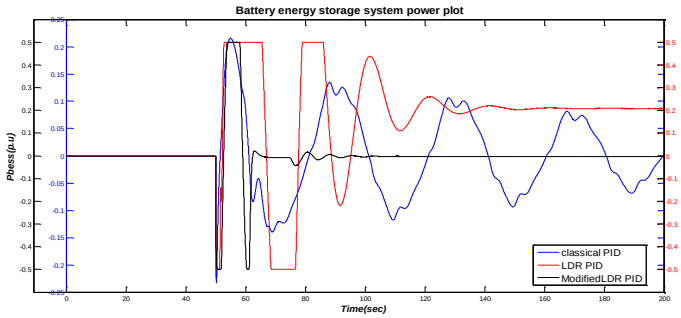

Figure 12(g). Contribution of BESS Power in Microgrid (Case 2)

From Figure 12(g) & Figure 12(h), we observed that the contribution of BESS and fly wheel is only for transient period. From the simulation results as obtained in Figure 18(a) -18(h), it is shown that the dynamic behavior of the proposed system gives better output as compared to the classical method and LDR method.

Case 3: Wind power decreases from 0.3 p.u. to 0.25 p.u. and again increases from 0.25 p.u. to 0.28 p.u. & solar power is decreased from 0.3 p.u. to 0.25 p.u. and again decreases to 0.20 p.u. similarly load demand is first decreased from 0.6 p.u to 0.55 p.u and then increased to 0.70 p.u. for a time period of 50 sec. and 100 sec. respectively.

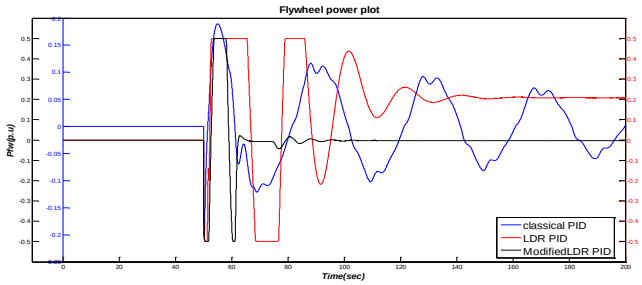

Figure 12(h). Contribution of Fly Wheel Power in Microgrid (Case 2)

Time	T=0 sec	T=50 sec	T=100 sec
Wind power	0.3 p.u.	0.25 p.u.	0.28 p.u.
Solar power	0.3 p.u.	0.25 p.u.	0.20 p.u.
Load demand	0.6 p.u.	0.55 p.u.	0.70 p.u.

In this study, we consider supply and load both are varying simultaneously for 2 time intervals. Simulation results are shown in Figure 13(a) -13(h).

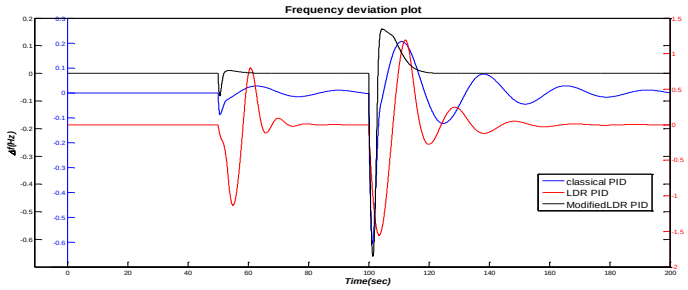

Figure 13(a). Frequency Deviation of Microgrid (Case 3)

From Figure 13(a), the following observation can be observed. For classical method, the first transiet is not eliminated and the second transient is eliminated in 160 sec. For LDR method, the first transient is eliminated in 35 sec and the second transient is eliminated in 100 sec. For Modified LDR method, the first transient is eliminated in 12 sec and the second transient is eliminated in 22 sec for frequency regulation.

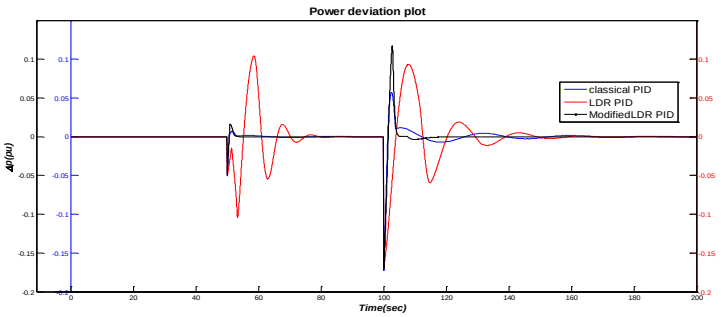

Figure 13(b). Power Deviation of Microgrid (Case 3)

From Figure 12(b), the following observation can be observed. For classical method, the first transient is 40 sec. and the second transient is eliminated in 130 sec. For LDR method, the

first transient is eliminated in 35 sec and the second transient is eliminated in 90 sec. For Modified LDR method, the first transient is eliminated in 12 sec and the second transient is eliminated in 22 sec. for regulation of power.

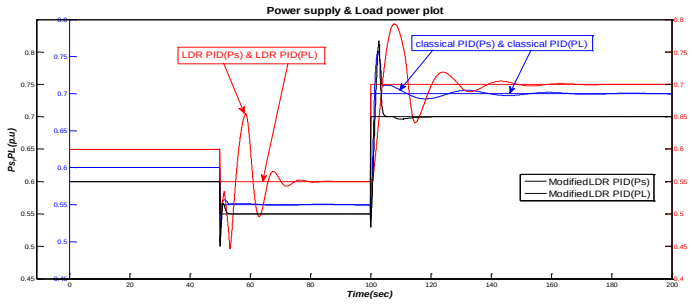

Figure 13(c). Supply Power and Load Power of Microgrid (Case 3)

From figure 13(c) we observe that, the Modified LDR gives faster response as compared to LDR and classical methods.

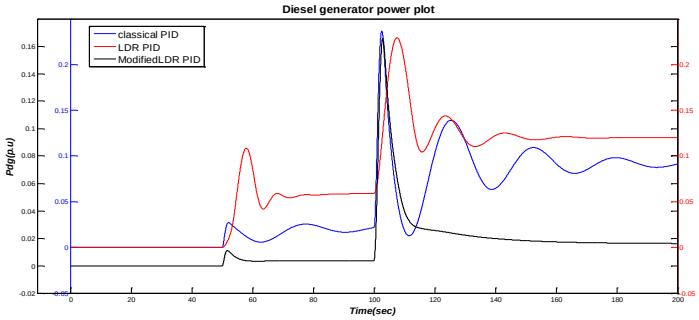

Figure 13(d). Contribution of Diesel Generator Power in Microgrid (Case 3)

At steady state period, contribution from diesel generator is 0.1 p.u at 150 sec, 0.12 p.u at 80 sec and 0.02 p.u at 75 sec for Classical, LDR and Modified LDR method respectively to compensate the difference in load power of 0.22 p.u. This has been shown in Figure 13(d).

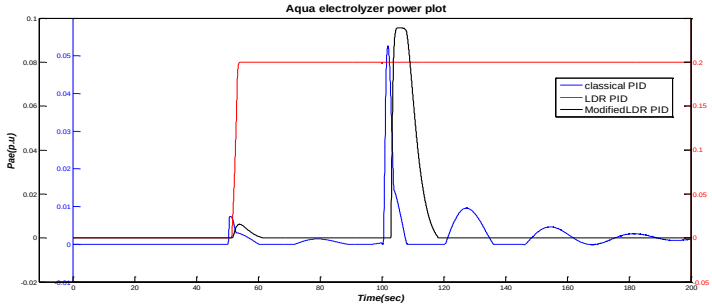

Figure 13(e). Contribution of Aqua Electrolyzer Power in Microgrid (Case 3)

The contribution of Aqua electrolyzer is negligible, it is used to generate Hydrogen for fuel cell only. This has been shown in Figure 13(e).

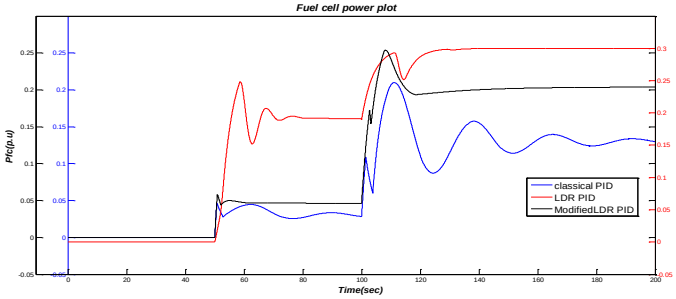

Figure 13(f). Contribution of Fuel Cell Power in Microgrid (Case 3)

From Figure 13(f), the fuel cell is contributing 0.12 p.u. power in 200 sec for classical method whereas 0.30 p.u. in 30 sec and 0.2 in 70 sec for LDR method and Modified LDR method respectively to compensate the difference in load power of 0.22 p.u. for frequency regulation.

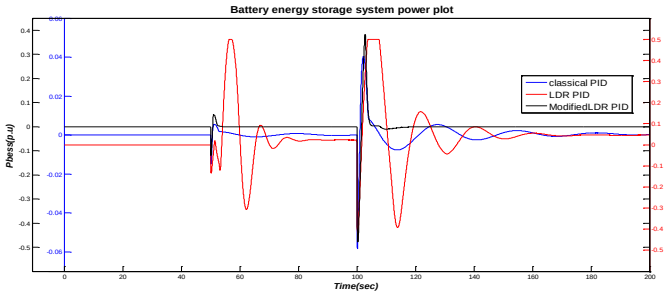

Figure 13(g). Contribution of BESS Power in Microgrid (Case 3)

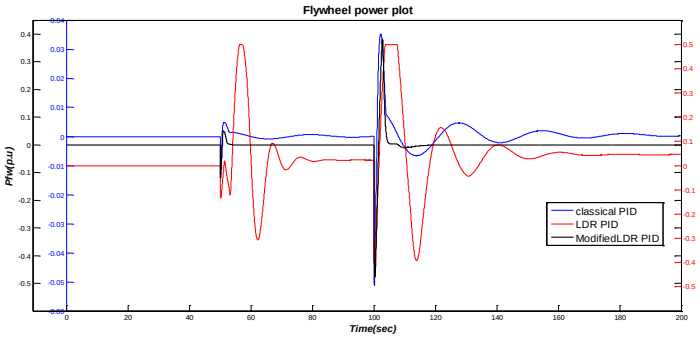

Figure 13(h). Contribution of Fly Wheel Power in Microgrid (Case 3)

From Figure 13(g) & Figure 13(h), we observed that the contribution of BESS and Fly wheel is only for transient period.

From the simulation results as obtained in Figure 13(a)-13(h), it is shown that the dynamic behavior of the proposed system gives better output as compared to the classical method and LDR method.

5. Conclusion

A comparison of Modified LDR, LDR and classical PID based approaches shows the superiority of proposed Modified LDR over LDR and classical PID for three different cases. Thus the Modified LDR based PID controller has better dynamic response i.e., quick in

operation, reduced error magnitude and minimized frequency transients. The simulation results obtained and tabulated in Table 1, 2 and 3 shows that the proposed Modified LDR based controllers tracks the load changes and achieve good robust performance than classical PID and LDR based PID controller.

The most important contribution of the research work presented in the paper work is Modeling of microgrid. Tuning of controller parameter gain using LDR technique. Design of p-f droop based on bode plot stability criterion.

References

[1] Chowdhury, SP, Crossley, P, Chowdhury, S, Clarke, E. 'Microgrids and active distribution networks' (Institution of Engineering and Technology, London, 2009)

[2] N Hatziargyriou, M Ddonnelly, S Papathanassiou, JA Pecas-Lopes, J Usaola, R Lasseter, A Efthymiadis, K Karoui, S Arabi, M Takasaki, H Chao, "Modeling new forms of generation and storage," *Electra*. 2001; (195): 54-63.

[3] Senjyo, T, Nakaji, T, Uezato, K, Funabashi, T. 'A hybrid power system using alternative energy facilities in isolated island', *IEEE Trans. Energy Convers.* 2005; 20(2): 406–414

[4] DJ Hall, RG Colclaser. "Transient modeling and simulation of a tubular solid oxide fuel cell," *IEEE Trans. Energy Convers.* 1999; 14(3): 749-753.

[5] MD Lukas, KY Lee, H Ghezel-Ayagh. "Development of a stack simulation model for control study on direct reforming molten carbonate fuel cell power plant," *IEEE Trans. Energy Convers.* 1999; 14(4): 1651-1657.

[6] PS Dokopoulos, AC Saramourtsis, AG Bakirtzis. "Prediction and evaluation of the performance of wind-diesel energy systems," *IEEE Trans. Energy Convers.* 1996; 11(2): 385-393.

[7] N Kodama, T Matsuzaka, N Inomata. "The power variation control of a wind generator by using probabilistic optimal control," *Trans. Inst. Elect. Eng. Jpn*. 2001; 121-B(1): 22-30.

[8] RB Chedid, SH Karaki, C El-Chamali, "Adaptive fuzzy control for wind-diesel weak power systems," *IEEE Trans. Energy Convers*. 2000; 15(1): 71-78.

[9] Lee, D, Wang, L. "Small signal stability analysis of an autonomous hybrid renewable energy power generation/energy storage system time domain simulations", *IEEE Trans. Energy Convers*. 2008; 23(1): 311–320.

[10] S Mishra, G Mallesham, AN Jha. "Design of controller and communication for frequency regulation of a smart microgrid," *IET Renew. Power Gener*. 2012; 6(4): 248–258.

[11] IJ Nagarath, M Gopal. Control Systems Engineering, 3rd Edition. New Age International: 2001.

[12] M Gopal. Control Systems Principles and Design, 3rd Edition. Tata Mc Graw Hill 2008.

[13] Mallesham, G, Mishra, S, Jha, AN. *'Ziegler- Nichols based controller parameter tuning for load frequency control in a microgrid'.* Proc. Int. Energy, Automation, and Signal (ICEAS), 2011 International Conference on. 2011; 1–8, 28-30.

[14] B Kroposki, R Lasseter, T Ise, S Morozumi, S Papathanassiou, N Hatziargyriou. "Making microgrid work," *IEEE Power and Energy Magazine*. 2008; 6(3): 40-53.

[15] RH Lasseter, "Microgrids," *Proc. IEEE Power Eng. Soc. Winter Meeting*, Jan. 2002; 1: 305-308.

[16] P Agrawal, *"Overview of DOE Microgrid Activities,"* Symposium on Microgrid, Montreal, June 23, 2006.

[17] O I Elgerd. Electric energy system theory: an introduction (2nd ed.), McGrawHill, New York (1982).

[18] P Kundur. Power system stability and control, Tata McGraw Hill, New York, 1994.

[19] Dulal ch. Das, AK Roy, N Sinha. *"Genetic Algorithm Based PI controller for frequency control of an autonomous hybrid generation system",* IMECS Hong Kong. 2011; 2, march 16-18. MATLAB 7.10.0 (R2010a).

[20] Majumder, R Chaudhuri, B Ghosh, A Majumder, R Ledwich, G Zare, F. "Improvement of stability and load sharing in an autonomous microgrid using supplementary droop control loop,"*Power and Energy Society General Meeting, 2010 IEEE*, vol., no., pp.1,1, 25-29 July 2010.

[21] Diaz, G Gonzalez-Moran, C Gomez-Aleixandre, J Diez, A, "Scheduling of Droop Coefficients for Frequency and Voltage Regulation in Isolated Microgrids," *Power Systems, IEEE Transactions on*. 2010; 25(1): 489, 496.

[22] CSA Nandar. "Robust PI control of smart controllable load for frequency stabilization of microgrid power system," *International Journal of Renewable Energy*. 2013; 56: 16-23.

[23] J Schiffer, R Ortega, A Astolfi, J Raisch, T Sezi. "Conditions for stability of droop-controlled inverter-based microgrids," *International Journal of Automatica*. 2014; 50(10): 2457-2469.

[24] MA Zamani, TS Sidhu, A Yazdani. "A communication-based strategy for protection of microgrids with looped configuration," *International Journal of Electric Power Systems Research*. 2013; 104: 52-61.

APPENDIX

Nominal parameters of the microgrid [10]

f_{sys}=50 Hz, P_{base}=1 MVA, D = 0.012 MW/Hz, H = 5 s, $T_{dg}=2$ s, $T_{dt}=20$ s, T_{fc}=4 s, T_{ae}=0.2 s, T_{BESS}=0.1 s, T_{fw}=0.1S, $K_{dg}=K_{dt}=K_{ae}=K_{fc}=K_{BESS}=K_{fw}=1$

Nominal parameters of the microgrid [10]

Wind power source (300 KW), Solar Power source(300 KW), load(600 KW),Diesel Generator(400 KW), Fuel Cell(200 KW), Aqua Electrolyzer(100 KW), Battery(30 KWh) and Fly Wheel(30 KWh).

List of codes [20]

```
clc
[t1,w1,x1,x2,x3,x4,x5,x6,x7,x8,x9,x10,x11,x12,x13]=sim('classical',200);
[t2,w2,y1,y2,y3,y4,y5,y6,y7,y8,y9,y10,y11,y12,y13]=sim('LDR',200);
[t3,w3,z1,z2,z3,z4,z5,z6,z7,z8,z9,z10,z11,z12,z13]=sim('modifiedLDR',200);

%# Some initial computations:
axesPosition = [140 70 1100 530]; %# Axes position, in pixels
yWidth = 30; %# y axes spacing, in pixels
xLimit = [0 200]; %# Range of x values
xOffset = -yWidth*diff(xLimit)/axesPosition(3);

%# Create the figure and axes:
%Frequency Deviation
Figure(1)
h1 = axes('Units','pixels','Position',axesPosition,...
'Color','w','XColor','k','YColor','b',...
'XAxisLocation','bottom',...
'YAxisLocation','left',...
'XLim',xLimit,'YLim',[-0.7 0.3],'NextPlot','add');

h2 = axes('Units','pixels','Position',axesPosition+yWidth.*[-1 0 1 0],...
'XAxisLocation','bottom',...
'YAxisLocation','right',...
'Color','none','XColor','k','YColor','r',...
'XLim',xLimit+[xOffset 0],'YLim',[-2 1.5],...
'XTick',[],'XTickLabel',[],'NextPlot','add');

h3 = axes('Units','pixels','Position',axesPosition+yWidth.*[-2 0 2 0],...
'XAxisLocation','bottom',...
'YAxisLocation','left',...
'Color','none','XColor','k','YColor','k',...
'XLim',xLimit+[2*xOffset 0],'YLim',[-0.7 0.2],...
'XTick',[],'XTickLabel',[],'NextPlot','add');

L1=plot(h1,t1,x1,'b');
hold on
L2=plot(h2,t2,y1,'r');
hold on
L3=plot(h3,t3,z1,'k');
title(' Frequency deviation plot','fontname','timesnewroman')
xlabel(h1,'Time(sec)')
ylabel('\Deltaf(Hz)')
legend([L1,L2,L3],'classical PID','LDR PID','ModifiedLDR PID');
```